Article:

Bondar, D., Nanukuttan, S., Provis, J.L. et al. (1 more author) (2019) Efficient mix design of alkali activated slag concretes based on packing fraction of ingredients and paste thickness. Journal of Cleaner Production, 218. pp. 438-449. ISSN 0959-6526

https://doi.org/10.1016/j.jclepro.2019.01.332

Accepted Manuscript

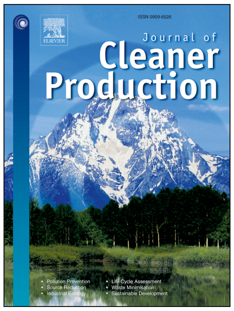

Efficient mix design of alkali activated slag concretes based on packing fraction of ingredients and paste thickness

Dali Bondar, Sreejith Nanukuttan, John L. Provis, Marios Soutsos

PII: S0959-6526(19)30365-8

DOI: https://doi.org/10.1016/j.jclepro.2019.01.332

Reference: JCLP 15719

To appear in: *Journal of Cleaner Production*

Received Date: 17 August 2018

Revised Date: 3 December 2018

Accepted Date: 30 January 2019

Please cite this article as: Bondar D, Nanukuttan S, Provis JL, Soutsos M, Efficient mix design of alkali activated slag concretes based on packing fraction of ingredients and paste thickness, *Journal of Cleaner Production* (2019), doi: https://doi.org/10.1016/j.jclepro.2019.01.332.

Efficient mix design of alkali activated slag concretes based on packing fraction of ingredients and paste thickness

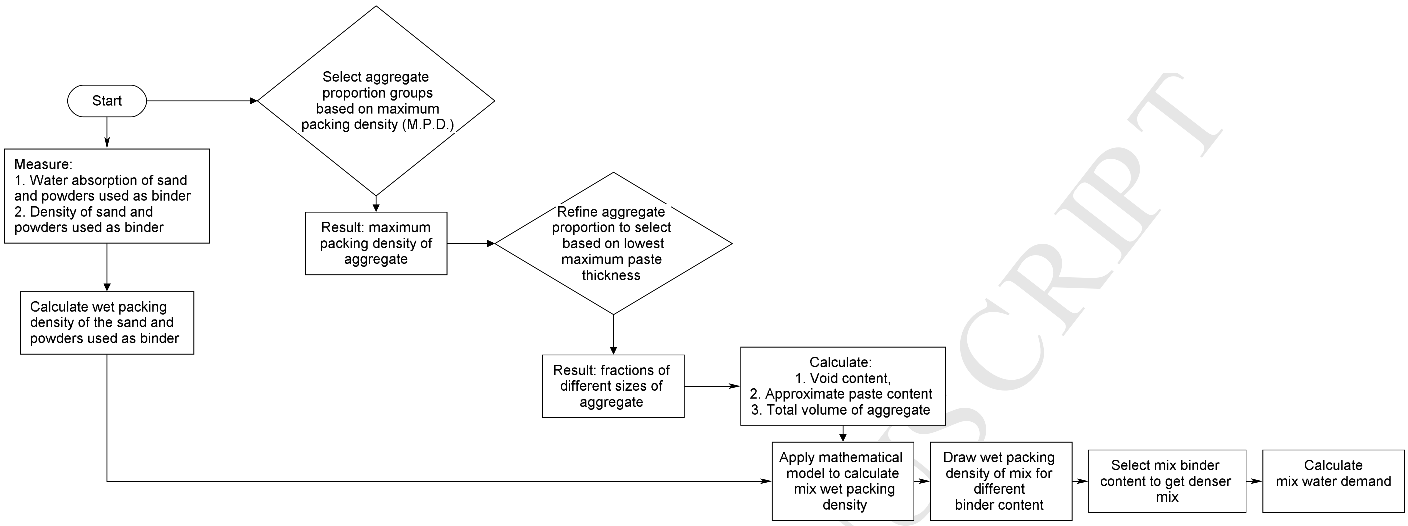

Efficient mix design of alkali activated slag concretes based on packing fraction of ingredients and paste thickness

Dali Bondar[1*], Sreejith Nanukuttan[1], John L. Provis[2], Marios Soutsos[1]

[1]School of Natural and Built Environment, Queen's University Belfast, Belfast BT9 5AG, UK

[2]Department of Materials Science and Engineering, University of Sheffield, Sheffield S1 3JD, UK

Email: dlbondar@gmail.com, s.nanukuttan@qub.ac.uk, J.Provis@Sheffield.ac.uk, m.soutsos@qub.ac.uk

Abstract

Many studies have been dedicated to the properties of alkali-activated slag concretes as a form of low-carbon high performance concrete, but less work has been focused on the application of mix design procedures to have a dense, durable and cost-efficient alkali-activated concrete. This study proposes a method for selecting the mix proportions of alkali-activated concretes based on the packing fraction of materials. The design method is based on the selection of the volumetric proportions of sand and coarse aggregate according to an ideal particle gradation curve. To validate this method, trial castings were carried out for concrete mixes containing alkali activated slag (AAS) with different paste contents to suggest the most cost-efficient concrete for different classes of workability and applications. Compaction and pore structure of these mixes studied by optical microscopy have shown that the design of AAS concretes based on the proposed method resulted in a dense and workable mix.

Keywords: Alkali activated slag concrete; efficient mix design; packing fraction

1 Introduction

The use of alkali activated materials as binders to produce concretes has gained increasing attention due to the need for emissions reduction, energy conservation and environmental considerations in the cement and concrete industry. Much work has been undertaken in optimising the chemistry of alkali-activated concretes made from different mineral resources and industrial by-products (Shi et al., 2006; Provis and Deventer, 2014; Bondar et al., 2011; Lloyd and Rangan, 2010; Bernal et al., 2011, 2012;

Pavithra et al., 2016; Yost et al., 2013; Ng and foster, 2013; Rafeet et al., 2017), but there is still the need for a rational mix design methodology which can be followed for fully efficient production of these concretes. In 2008, Lloyd and Rangan (2010) proposed a mix design method for alkali activated fly ash-based concrete but did not discuss how to deal with the effects of the ingredients' specific gravities, while assuming a constant concrete density of 2400 kg/m^3. As Shi et al. (2006) reported, the mix design methods presented for alkali activated slag concretes since 1967 are all based on experimental and empirical methods and need large amount of experiments and statistics to determine the relationship between the proportion of concrete constituents and the properties of concretes. Rafeet et al. (2017) published guidelines for mix proportioning of alkali activated fly ash/slag concrete, but there was no discussion on the density of concrete or how the fractions of aggregates with different particle size distributions affect the mix design. Li et al. (2018) recently reported a general mix proportioning method for alkali activated slag-based concretes considering highest bulk density of combined aggregates while the binder content was determined based on experimental method. The effect of compaction of wet ingredients and binder content was not considered in designing the mixture to get the possible highest density and minimum porosity.

The use of chemical activators in alkali-activated concretes also causes cost to be an issue when making alkali-activated concretes competitive with Portland cement-based concrete. McLellan et al. (2011) have shown that there is a wide variation in the calculated financial and environmental cost of geopolymers. Their study indicated potential for a 44-64% reduction in greenhouse gas emissions at financial costs between -7% and 39% higher than Portland cement, in the Australian context, depending on mix design. Thus, it is important to find the optimum paste content, based on optimal binder/aggregate and water/binder ratios, in alkali-activated concretes that can make workable concrete while meeting criteria for minimum strength grade and good durability.

Particle packing fraction measurements and particle packing models can help optimise the water demand and/or the paste content of concretes, while achieving a constant workability. In optimising the concrete composition by targeting a maximum particle packing fraction, the particle size distribution should be selected so as to fill the voids between large particles with smaller particles and to obtain a dense and interlocking particle skeleton in the resulting hardened concrete. In general, the higher the packing fraction of the aggregates, the smaller will be the volume of the voids to be filled by paste, and so less paste will be needed to provide sufficient excess over the void-filling material (Rafeet et al., 2017). It is this excess paste (above the paste needed to fill the voids between the aggregate particles) that lubricates the aggregate particles and enables the concrete to flow. Therefore, a higher packing fraction of the aggregates would at the same paste volume lead to a higher workability, or at the same workability allow the use of a smaller paste volume to increase the dimensional stability, paste consumption and carbon footprint (Li and Kwan, 2014; Kwan and Wang 2008; Domone and Soutsos, 1994; de Larrard and Sedran, 1994; Lange et al., 1997).

Moini et al. (2015) reported that the aggregate blends have considerable effect on concrete performance and as a result of aggregate optimisation, the concrete compressive strengths in their study increased by up to 37%; the improvement was slightly more pronounced at earlier age when the strength of the cementitious matrix is still low and concrete strength depends more on the load carrying capacity of the aggregates.

Zou et al. (2003) and Sutcu and Akkurt (2007) have also worked on packing of mono-sized and multi-sized mixtures and indicated that porosity of the assembly is strongly affected by particle size, their distribution and moisture content.

Recent work by Miller et al. (2016) has shown that concrete with a high water to binder ratio containing only cement as the binder provided a lower ratio of global warming potential (GWP) to compressive strength than some of the mixtures containing large quantities of replacement binder. This shows that large volume replacement of cement as a binder may not always be the most sustainable solution if mix designs are not optimised.

The aim of this paper is to build a consistent, rational and scientifically based approach for designing alkali activated slag concrete mixtures. Modern concretes for general use in engineering applications must meet a comprehensive list of requirements, which are not limited to the final compressive strength, but also include rheological properties, early age characteristics, deformability properties and durability aspects. Workability and compressive strength evolution were studied for mixes with different binder contents and water/binder ratios. Furthermore, the pore structures and microstructures of mixes were studied by optical microscopy to support the mix design approach.

2 Experimental programmes

2.1 Materials and methods of characterisation

The primary raw material used in this study is a granulated blast furnace slag which was supplied by ECOCEM, France (Table 1). The particle size distribution of slag was determined by laser diffraction, and the particle density was measured using a Le Chatelier flask; Fig. 1 and Table 2.

A centrifugal consolidation method was used to determine the actual water demand of slag (water absorption) according to the method Miller et al. (1996) suggested for measuring water demand of powders and fine particles based on achieving maximum packing density. In this method, 300 g of dry powder was mixed with a known content of water, in a 3 litre Hobart mixer, for 2 minutes at low speed. Then 50 g of this mix is poured into 90 mm long test tubes with internal diameter of 22 mm. By determining the mass of the paste in the test tube, the amount of the powder and water in the test tube at the beginning of the test were known. The test tube was then centrifuged for ten minutes at 4000 rpm in a Dumee Jouan E82N centrifuge with an internal diameter of 300 mm. The excess amount of water which came out as a supernatant layer on the top of the paste was removed with a pipette after centrifuging. By determining the amount of water removed, the amount of water absorbed was calculated and reported in Table 2.

Sodium hydroxide (NaOH) powder was dissolved in tap water and used along with sodium silicate solution (WG) to act as alkaline activators in concrete production at specified concentrations and compositions, as shown in Table 6. The chemical composition of the as-received sodium silicate solution was 15.5% sodium oxide (Na_2O), 30.5% silicon dioxide (SiO_2), and 54% water.

The aggregates used in this study were crushed basalt from local sources in Northern Ireland and comprised of 10 mm and 16.5 mm crushed fine and coarse aggregates and 4 mm sand complying with BS EN 12620 (2013). Sieve analysis of the aggregates is shown in Fig. 2. The bulk specific gravity and water absorption of these materials were measured based on BS EN 1097-1 and are presented in Table 3.

All size fractions of aggregates for the different mixes are presented in Fig. 3. The ingredients were mixed and filled into a 150mm diameter x 300 mm height cylindrical steel container in three equal layers. After filling each layer, the mixed aggregates in the container were compacted by applying 20 compaction blows with a metal tamper rod with diameter of 16 mm. The mass of the compacted mixed aggregates was measured, and the bulk dry packing fraction (refer to Table 4) was determined for the compacted mixed aggregates using the following equation:

$$\gamma = \frac{4W}{\pi\, D^2 (H - \delta H)} \qquad (1)$$

Where γ is the bulk dry packing density of compacted mixed aggregates (kg/m^3), W is the mass of compacted mixed aggregates (kg), H and D are the height and diameter of the container (m), and δH is the height reduction due to compaction of materials (includes the three individual differences in height), m.

Compacted dry packing fraction of mixed aggregate (φ) were determined by the following equation:

$$\varphi = \gamma . \sum_{i=1}^{n} \frac{A_i}{P_i} \qquad (2)$$

Where P_i is the grain density (bulk specific gravity) of the aggregate fraction (kg/m^3), A_i is the fraction of the aggregate (mass %) and n is the number of aggregate fractions. The results of this analysis are presented in Table 4.

For measuring the wet packing fraction of crushed aggregate fractions individually (i.e., 5-10 mm and 10-16.5 mm), the wet aggregates (saturated aggregates with moisture on the surface) were filled separately into a steel container in three equal layers. Each layer was compacted by applying 20 compaction blows with a metal tamping rod before progressing to the next layer. The weight of the container with and without the aggregates and the volume of space filled by the aggregate was measured and was used to determine the bulk wet packing fraction.

2.2 Mixing

All the concrete ingredients were mixed in a laboratory pan-mixer according to the formulations in Tables 5 and 6. Crushed basalt aggregates and sand were dry-mixed together for a minute; after adding the granulated blast furnace slag (GGBS) powder, mixing continued for 2 minutes and then the sodium hydroxide solution was added and after 2 minutes further mixing, sodium silicate solution was added and mixing continued for a minute.

2.3 Measuring fresh properties

The slump value and flow test were measured according to Part 2 and Part 5 of BS EN 12350 (2009), respectively. The mixes studied here span from highly fluid to very stiff, both tests were conducted for each mix, but the slump data are more instructive for moderate to stiff concretes, while slump flow is more useful for highly flowable mixes where the measured slump values are very high.

The wet (fresh) density of each mix, was measured based on the weight and volume of fresh concrete immediately after filling the two cube moulds in three equal layers and vibrating them at each time.

2.4 Casting and curing of the specimens

From each concrete mix, nine 100 mm cubes were cast, and used for the determination of compressive strength according to BS EN 12390-3 (2009) at 2, 7, 28 and 90 days of age, with two replicate samples tested per age; the remaining cube sample from each mix was used for preparing thin section samples as described below. The density of each mix was measured based on the weight and volume of the cubes cast for measuring compressive strength before crushing them. The concrete specimens were cast in three equal layers and compacted on a vibrating table. After casting, all the specimens in mould were covered with plastic sheets and left in the casting room for 24 hrs. Thereafter, the samples were removed from the mould and kept in plastic zip bags at 20°C until the test date.

The cube from each set that was not used in compressive strength testing was cured for 90 days, at which time material was sampled from its centre to be prepared for thin section samples. For preparing thin section samples, following impregnation with blue dye resin and drying, the back of the specimen was glued to a glass plate. Then the selected face of the concrete specimen was prepared by dry grinding and mounted on the glass slide. The thin section optical microscopy was used to study the pore structure of all of these mixes.

3 Results and discussions

The basis of the mix designs used in this study is a standard concrete mix being used in the round-robin testing programme of RILEM Technical Committee 247-DTA[1] (2014), which was designed to target a relatively low activator content for making structural concrete from alkali activated slag. In the RILEM TC 247-DTA mix design, oven-dried rounded quartz aggregates had been used, yielding flowable concretes, while crushed basalt aggregates were available for use in this work. The first trial mixes (Table 5) showed that even by increasing the water/binder (W/B) ratio from 0.45 to 0.5, no workability could be achieved with crushed basalt aggregates. So, workability of the mixes appeared to be an issue which was addressed through the following steps:

- Increasing the ratio of coarse to fine aggregates
- Decreasing the aggregate to binder (A/B) ratio.
- Considering the water absorption of materials based on saturated surface dry conditions, to add extra water required for both hydration and workability.
- Increasing the sodium silicate dose by 1% (relative to the mass of slag) and comparing the workability and strength results.

The first three of these items can be met reasonably by considering the packing fraction of the particles and the paste thickness needed to reach to a cost efficient dense workable mix design. The packing fraction of the mixture is defined as the solid volume of (aggregate) particles in a unit volume, which is optimised by mixing different fractions of particles with a view to minimise the porosity, which allows the use of the least possible amount of paste. However, this must be balanced with the provision of sufficient paste thickness to give suitable flow characteristics.

3.1 Selection of aggregate proportioning based on packing fraction and paste thickness

For considering aggregate proportions with maximum packing fraction in the mix design, different fractions of sand and crushed aggregates were selected, optimising away from the simple blend fractions used in the baseline mix design (Fig. 3). The results are presented in Fig. 4 and show that the maximum packing fraction (resulted from equation 2 for different fractions of aggregates mixes) is 0.68 for the three aggregate proportions: 40:12:48, 40:18:42, and 50:25:25 (Mass fractions reported as sand:10 mm:16.5 mm). Based on these results, void content (VC) will be $(1\text{-}\varphi) = (1-0.68) = 0.32$. The volume of the cement paste must be more than the void space between particles to overfill them after compaction. Thus paste content (PC) will be 10% in excess of void content (Raj et al., 2014) (1.1xVC) = (1.1X0.32) =0.352. The total solid volume content (TSVC) of aggregate for the above three aggregate proportions was calculated by the equation below:

$$\text{TSVC}=\sum_{i=1}^{n} A_i \,/\, P_i \qquad (3)$$

[1]https://www.rilem.net/groupe/247-dta-durability-testing-of-alkali-activated-materials-290

and the mass of each type of aggregate per cubic meter was thus calculated as $\left[\frac{(1-PC)}{TSVC} \cdot A_i . 1000\right]$. The minimum required binder content was calculated for different water/binder (W/B) ratios (1000PC/(W/B+1/ρ_{binder}), Table 7.

De Larrard (1994) has investigated in more detail the variations of concrete compressive strength, with the topology of the aggregate skeleton as the primary parameter and showed that the second key parameter governing the concrete compressive strength is the maximum paste thickness (MPT). He mentioned that this physical parameter represents the mean distance between two aggregates, if each aggregate is surrounded by a paste layer whose thickness is proportional to the aggregate diameter, equation 4:

$$e_M = D(\sqrt[3]{g^*/g} - 1) \qquad (4)$$

Where e_M is the MPT, D is the maximum size of aggregate, g^* is the packing fraction of the aggregate and g is the actual volume of the aggregate in the mix (de Larrard and Sedran, 1994). For the above aggregate mix proportions with maximum packing fraction (= 0.68), the maximum paste thicknesses are 3.711, 3.729 and 3.747 mm for aggregate proportion 40:12:48, 40:18:42, and 50:25:25, respectively. Due to the use of a crushed basalt aggregate in this study, these values are selected to be at the top end of the range 0.61 to 3.83 mm which Torres et al. (2015) have presented as maximum paste thicknesses for normal concrete at the highest compaction level and the lowest paste content.

The lowest maximum paste thickness belongs to aggregate proportion 40:12:48 (Sand: 10 mm: 16.5 mm).

Several particle packing models have been developed over the past decades and applied to concrete mix design. Andreasen (1930) developed a packing theory based on continuous particle distributions. The equation he derived, the Andreasen equation for dense packing, is $F_v(a) = (a/a_{max})^n$ where $F_v(a)$ is the cumulative finer volume distribution, and a_{max} is the maximum particle size. Andreasen's experiments indicated that to obtain a dense packing, n must be 0.33 to 0.50. The Andreasen equation indicates that infinitely small particles are required to achieve the theoretically denser packing. For real particle system, the minimum particle size is limited. Dinger and Funk recognized that real particle systems must have some minimum particle size (a_{min}) (Andreasen, 1930; Zheng et al., 1990; Jones and Zheng, 2002). They modified the Andreasen equation to indicate a size range a_{max} to a_{min} and a cumulative finer fraction of zero when $a = a_{min}$:

$$F_v(a) = (a^n - a_{min}{}^n) / (a_{max}^n - a_{min}^n) \quad (5)$$

A study on four particle packing models used to proportion the mix constituents (solid particles) of concrete to produce a minimum voids ratio (or maximum packing fraction) was published by Jones et al. (Jones et al., 2002). It was found that the models give broadly the same output and suggest similar combinations of materials to give the minimum voids ratio. It was noted that proportioning concrete mix constituents to minimise voids ratio did tend to produce a harsher and unworkable mix than normal (Jones et al., 2002).

Validation was performed with Elkem Emma® software incorporating the modified Andreasen model. For each aggregate proportion i.e. 40:12:48, 40:18:42, and 50:25:25 and a constant paste volume, by decreasing the binder content and increasing the water to binder ratio the density has been reduced (Table 7). By using finer crushed aggregates and more sand in the aggregate mixtures the density has been increased a little, but on the other hand there is a certain probability that voids may be trapped under an aggregate. More precisely, the fractions which may lead to entrapment of the air bubbles are the ones that have simultaneously a sufficient particle size and a high specific surface (de Larrard, 1999). Therefore, the sand fractions are the most efficient at retaining air, while the cement paste cannot fix a significant amount of entrapped air in the absence of air entraining admixtures, which were not used here. Furthermore, the water content of sand at saturated surface dry conditions is generally much higher than that of crushed aggregates, so the likelihood of changes in concrete water content will be higher. Finally, the more sandy the mixture, the more sensitive will be the strength to changes in workability (de Larrard, 1999). The effect of air content on slump greatly increases with the sand content of the mixture and this air content will in turn affect the compressive strength. Thus, considering the above description and the least maximum paste thickness, the aggregate proportion 40:12:48 was used for the mixes in this study.

3.2 Selection of mix binder content based on wet packing fraction (WPF)

The wet packing fraction (WPF) of slag, sand, crushed fine and coarse aggregates were measured separately, and these values were used to calculate the total WPF of the mixture with different binder (slag) contents based on Goltermann et al. (1997), these are presented in Table 8. It is known that the WPF of fine particles such as slag and sand is inversely proportional to water/powder ($\frac{w}{p}$) at the same fluidity (Zou et al., 2001; Ye et al., 2008). The higher the WPF, the smaller will be the water to powder (or water to fine particle) ratio. This is because higher packing fraction leads to less pores, so smaller amount of paste is needed and cause smaller water to powder ratio which is direct proportional to the paste content. In equation 6, ρ' and (1-ρ') are the volume fractions occupied respectively by powder (or fine particle) and water in the paste (or mix), which represent the WPF and the void content (Ye et al., 2008). If the true densities of water and particles are ρ_w and ρ_p, the relationship between water to powder (or water to particle) ratio and wet packing fraction (WPF=ρ') can be written:

$$\frac{w}{p} = \rho_w(1-\rho')/(\rho_p\ \rho') \qquad (6)$$

and WPF could be obtained from the water to particle ratio which is measured at the least fluidity for samples with different particle size distribution (Ye et al., 2008; Miller et al., 1996). Using equation

(6) and $(\frac{w}{p})$ ratio measured by centrifugal consolidation method (0.35 for slag and 0.178 for sand), the WPF of slag and sand was found to be 0.499 and 0.674 respectively. For the two different size fractions of crushed aggregates (5-10 mm and 10-16.5 mm), WPF was measured 0.536 and 0.548. Then using Golterman et al. (1997), WPF was calculated for mixed coarse crushed aggregates without and with sand, to be equal to 0.565 and 0.636 respectively. Further, the total WPF for mixes with different binder contents was calculated, Table 8. Fig. 5 shows that maximum packing fraction is obtained for 350 kg/m^3 of GGBS and the value remains constant up to 450 kg/m^3. The WPF decreased for mixes with binder content greater than 450 kg/m^3.

The total volume of aggregates and binder of the mixes, calculated as described above, is used to find the mix water demand. The steps required to select mix proportions for a mix are shown in Fig. 6 as a flow chart.

3.3 Density, slump, flow and compressive strength

Slump, flow, density and compressive strength were measured for all the five groups of mixes presented in Table 6. The test variables were binder content and water content, and their influence on slump, flow, density and compressive strength was assessed in order to validate the mix design procedure based on a particle packing approach. Testing these mixes shows the best combination of binder and water content at the same paste volume for a strong and workable mix.

3.3.1 Density

Fig. 7 shows that for mixes with W/B of 0.45, the highest wet concrete density correspond to the mixes with binder content from 437.7 to 450 kg/m^3, with a maximum of 2482.7 kg/m^3 at a binder content of 447.6 kg/m^3. At W/B = 0.55 this will happen for mixes with binder content from 365.1 kg/m^3 to 414.6 kg/m^3 with a peak of 2439.5 kg/m^3 at 398.1 kg/m^3. Increasing water binder ratio to 0.65, this is resulted for mixes with binder content from 315.6 kg/m^3 to 375 kg/m^3 with a maximum of 2436.6 kg/m^3 at a binder content of 351.9 kg/m^3. These results confirm previous calculation results presented in Table 7 where the calculated binder content based on packing fraction and paste thickness method for mixes with water/binder equal to 0.45, 0.55 and 0.65 was resulted 440, 391.11 and 352 kg/m^3 respectively. Density measurement results show that at W/B of 0.65 mixes with a binder content of 350 kg/m^3 has shown the highest density at different ages up to 28days (Fig. 8c). Furthermore, with regarding to the results is shown in Fig. 8a&b, at W/B of 0.45 and 0.55, mixes with a binder content of 450 kg/m^3 and 400 kg/m^3 has shown the highest wet concrete density.

Fig. 8 depicts that density reduces with increase in W/B, this is to be expected as more water is present in the matrix. It is also obvious that density reduces with age because of water evaporation due to the semi-dry (sealed) curing condition which was used to prevent leaching of alkalis due to water curing. This reduction is more obvious for mixes with higher binder content due to the fact that they have a higher quantity of water that can evaporate. This evaporation is likely to result in a more porous concrete. In addition, minimum variability as the difference between the three replicates occurred for mixes with W/B of 0.55, and as binder content reduces the wet density decreases for low W/B concrete, but this trend reverses for high W/B concrete.

The lowest density is observed for mixes with binder content equal to 400 kg/m^3 and 450 kg/m^3 and water to binder ratio equal to 0.65 for all ages (Fig. 8). When the fraction of aggregate and paste are considered based on packing fraction (lower void content) then less difference can be observed between the density of these mixes compare to the mixes with lower binder content.

3.3.2 Slump and flow

AASC has often been known for its relatively low slump value and rapid setting behaviour. Slump values of 60-120 mm have been reported in the literature (Collins and Sanjayan, 1999). The purpose of this testing programme was to demonstrate the effect of mix design based on packing fraction on the slump value that AASC is capable of producing, and to identify the governing W/B and binder content that are necessary to achieve high slump. As is evident from Fig. 9 and 10, for a given W/B, the drastic change of slump and flowability happens at the binder content calculated based on the mix design with highest packing fraction method (i.e. for W/B=0.55, is at 400 kg/m^3). For mixes with water to binder ratios of 0.45 and 0.55, the minimum binder content required to produce a workable mix is 450 and 400 kg/m^3, respectively.

The use of sodium silicate as a dispersant is reported to reduce the yield stress of a paste considerably, to obtain good workability (Landrou et al., 2016). Fig. 9 shows that adding 1% more sodium silicate to increase the slump is not effective when water to binder ratio is equal to 0.45, but at higher W/B, it is more effective and increases the slump from 100 mm to 230 mm and 225 mm to 250 mm, for the mixes with water to binder ratio of 0.55 and 0.65, respectively.

The contour map graphs in Fig. 14 (a) show slump as a function of binder content and water to binder ratio, for different mixes with the same activator content. As it can be observed, a water to binder ratio equal to 0.55 seems to be the minimum amount of W/B in order to achieve all classes of workability by varying binder content from 350 to 450 kg/m^3.

3.3.3 Compressive strength

The mechanical and durability properties of concrete are highly influenced by its density (Bondar et al., 2018). A denser concrete provides higher strength and fewer amount of voids and porosity. Fig. 11 and 12 show the relation between the density of the mixes and their compressive strength at different ages. Compressive strength of samples at different age has a good linear correlation with wet density (Fig. 11) and with dry density (Fig. 12).

An overall comparison of the results for different W/B (Fig. 13) makes the effect of W/B very apparent for all the mixes. Whereas mixes with W/B of 0.45, 0.55 and 0.65, offers the minimum value of strength around 22, 11 and 10 MPa at 2 days and 42, 29 and 24 MPa at 90 days. The highest compressive strengths are observed for mixes with water to binder ratio equal to 0.45: in the range of 22-26 MPa at 2 days and 42-49 MPa at 90 days. Increasing the sodium silicate dose by 1%, with the aim of increasing the workability, decreases the compressive strength 29% at early ages and up to 17% at longer ages (Fig. 13(b)).

Wasserman et al. (2009) reported that strength of Portland cement (PC) based concrete is a function of w/c and independent of the cement content. This is also true for AASC; comparing different mixes tested at the same age and with same water to binder ratio shows that increasing the binder content has no major effect on strength. For W/B = 0.55, increasing binder content to more than 350 kg/m^3 cannot produce significantly higher compressive strength. Therefore, increasing the cementitious material content will not in itself guarantee higher strength, although mixes with binder content less than 400 kg/m^3 do not offer good workability. For lower binder contents, the mix is not workable and the voids content increases in concrete and makes them more porous. Fig. 14 can be used to design alkali activated slag concrete mixtures using similar aggregates to those used in this study, with the lowest content of chemical activators for practical applications. It shows that to achieve the minimum value of the slump class of S2 (50 mm) specified in BS EN 206 (2013) the minimum water to binder ratio and binder content are 0.5 and 400 kg/m^3 respectively.

3.4 Pore structure

Thin sections were prepared from all twelve concrete samples as they represent alkali activated slag concrete mixes with different binder to aggregate ratio (binder content) and water to binder ratio. Fig. 15 shows all twelve thin section images taken at a magnitude of 5^X from these samples. A narrow zone of cement paste with a high porosity and/or cracks is occasionally seen at the interface between the coarse aggregate particles and the surrounding hardened binder paste in some of them, which can be due to a water concentration gradient based on heterogeneity close to the aggregate (San Nicolas and Provis 2015) (Fig. 15 d, g, h & k). Furthermore, the coarse aggregate particles also exhibit signs of internal cracking (Fig. 15 c & f). Concrete is a three-phase material, in which the gaseous phase can never be totally removed. The images in the same row in Fig. 15 show samples with same binder content and different water to binder ratios, while the images in each column present mixes with same water to binder ratio and different binder content. It can be observed that mixes with water to binder ratio of 0.45, 0.55 and 0.65, a corresponding binder content of 450, 400 and 350 kg/m^3 result in a dense matrix. Indeed, the density is a good indicator that reflects the durability of concrete. However, the size distribution and the sinuosity of pores can also effect the durability of concrete. Image analysis was performed by image analysis software (Image Pro) and the void contents in the concrete including percentage of pores in the binder, were measured by counting pixels in area of interest with the same colour scale (or intensity) of that of the micro cracks observed in some of the specimens, divided by the whole pixels in the same area of interest and presented in Fig. 16. At W/B of 0.45, 0.55 and 0.65, the least pore percentage was resulted for mixes with binder content of 450, 400 and 350, respectively. Therefore, these results confirm the mix design method and show that these mixes can present least porous matrixes which will have better durability properties for this new type of concrete.

Conclusions

This article shows that a rational mix design for alkali activated material (AAM) concretes can be achieved based on optimising packing fraction of the ingredient particles and giving consideration to the minimum required paste thickness to coat the aggregates for workability.

1. Alkali activated slag concretes designed in this way yielded higher slump for a given water content.
2. For each water to binder ratio there is an optimum amount of binder required; increasing the binder content beyond this point will not contribute to strength but will increase the workability, while mixes with less binder content are not workable.
3. AAS concretes with a minimum dosage of activators can be designed for different classes of workability and concrete strength grades from C16/20 to C32/40.
4. Typically, AAS concretes with a minimum dosage of activator require a binder content of 400 kg/m^3 and water/binder ratio of 0.55, to provide a cost-efficient workable normal C25/30 concrete.
5. The binder contents selected in alkali activated slag concrete mixes designed based on wet packing fraction to get minimum water content are realistic, and do not cause high evaporation with the associated consequences of making large pores in the concrete. However, increasing the binder content can give a more porous structure for the product overall.

Acknowledgements

This work was supported by the United Kingdom Engineering and Physical Sciences Research Council (EPSRC) under grant EP/M003272/1, awarded jointly with NSFC (China).

Table 1: Oxide composition of GGBS used, from X-ray fluorescence analysis

Material	Component (mass% as oxide)

	SiO_2	Al_2O_3	CaO	Fe_2O_3	MgO	TiO_2	Other	LOI*
GGBS	35.7	11.2	43.9	0.3	6.5	0.512	1.578	0.31

* LOI is loss on ignition at 1000^0C.

Table 2: Physical properties of GGBS

Fineness (particles ≥45 µm)	7.74%
Particle density (tonnes/m^3)	2.86
Water absorption	35.14%

Table 3: Physical properties of aggregates

Aggregates	Bulk specific gravity	Bulk Saturated surface dry (SSD) Specific gravity	Water Absorption (%)
Sand (0-4 mm)	2.72	2.73	0.75
Crushed Agg.(5-10 mm)	2.67	2.75	3.14
Crushed Agg.(10-16.5 mm)	2.60	2.67	2.60

Physical properties of sand and crushed aggregates were measured based on BS EN 1097-1.

Table 4: Bulk and compacted packing fraction for various aggregate proportions

Aggregate proportions (Sand/10mm/16.5mm)	Bulk packing fraction (kg/m^3)	Compacted packing fraction
20/16/64	1.618	0.614
20/24/56	1.616	0.612
20/32/48	1.612	0.609
30/14/56	1.736	0.560
30/21/49	1.736	0.655
30/28/42	1.735	0.653
40/12/48	1.805	0.680
40/18/42	1.801	0.677
40/24/36	1.781	0.669

50/25/25	1.828	0.683

Table 5: Baseline mix design and initial trial mixes for AASC

Mix No.	GGBS (kg/m^3)	NaOH (%)	WG (%)	Sand (kg/m^3)	Crushed Agg. (kg/m^3)	Blend ratios Sand/Fine Cr Agg. / Coarse Cr Agg.	W/B	Slump (mm)	Compressive strength (MPa)	
									7 days	28 days
Baseline-1*	320	4	6	756	1134	40-24-36	0.45	0	37.1	45.1
2*	320	4	6	756	1134	40-24-36	0.5	0	27.8	37.9

*For these mixes Na_2O=2.775%, SiO_2/Na_2O ratio (Ms) =0.324 and A/B=5.9

Table 6: Alkali activated slag concrete mixes with different binder content and water to binder ratio for validation of mix design method

Mix Group No.	GGBS (kg/m^3)	Na(OH) (kg/m^3)	Na silicate (kg/m^3)	Sand (kg/m^3)	Crushed Agg.(5-10mm) (kg/m^3)	Crushed Agg. (10-16.5mm) (kg/m^3)	Water (kg/m^3)-W/B	Paste content	Excess of paste content to void content	Aggregate Mix proportion	Aggregate to binder ratio	90 days density (kg/m^3)
MG1	300	12	18	822	247	986	135-0.45	0.24	-0.25	40-12-48	6.85	2415
	300	12	18	789	237	947	165-0.55	0.27	-0.16	40-12-48	6.58	2410
	300	12	18	757	227	908	195-0.65	0.30	-0.06	40-12-48	6.31	2392
MG2	350	14	21	778	234	934	157.5-0.45	0.28	-0.12	40-12-48	5.56	2410
	350	14	21	741	222	889	192.5-0.55	0.32	-0.01	40-12-48	5.29	2400
	350	14	21	703	211	843	227.5-0.65	0.35	0.09	40-12-48	5.02	2367
MG3	400	16	24	735	221	882	180-0.45	0.32	0.00	40-12-48	4.6	2380
	400	16	24	692	208	830	220-0.55	0.36	0.13	40-12-48	4.33	2393
	400	16	24	649	195	779	260-0.65	0.40	0.25	40-12-48	4.05	2314.5
MG4	400	16	28	735	221	882	180-0.45	0.32	0.00	40-12-48	4.6	2365

	400	16	28	692	208	830	220-0.55	0.36	0.13	40-12-48	4.33	2377
	400	16	28	649	195	779	260-0.65	0.40	0.25	40-12-48	4.05	2354
MG5	450	18	27	692	208	830	202.5-0.45	0.36	0.13	40-12-48	3.84	2390
	450	18	27	643	193	772	247.5-0.55	0.41	0.27	40-12-48	3.57	2354
	450	18	27	595	178	714	292.5-0.65	0.45	0.41	40-12-48	3.30	2310

Table 7: Theoretical mix design based on maximum packing fraction of aggregates

Mix No.	Aggregate proportion (Sand/10mm/16.5mm)	Aggregate packing fraction	Total solid volume of aggregate	Sand (kg/m^3)	Crushed Agg. (5-10mm) (kg/m^3)	Crushed Agg. (10-16.5mm) (kg/m^3)	W/B	Theoretical GGBS content (kg/m^3)	Density calculated by Emma Software (kg/m^3)
1	40-12-48	0.68	0.370	700.54	210.16	840.65	0.45	440	2.39
							0.55	391.11	2.36
							0.65	352	2.33
2	40-18-42	0.68	0.369	702.44	316.10	737.56	0.45	440	2.39
							0.55	391.11	2.36
							0.65	352	2.34
3	50-25-25	0.68	0.368	880.44	440.22	440.22	0.45	440	2.4
							0.55	391.11	2.37
							0.65	352	2.34

Table 8: Wet packing fraction of different mixes to get minimum water demand

Mix specification	Mixture ingredients properties	Slag	Sand	Fine Crushed	Coarse Crushed	Total wet packing fraction (WPF)
	Density (kg/m^3)	2.86	2.73	2.75	2.67	
	Wet packing fraction	0.499	0.674	0.536	0.548	
Mix 100GGBS	Mass (kg)	100	701	210	841	0.638
	Volume fraction	0.051	0.376	0.112	0.461	
Mix 200GGBS	Mass (kg)	200	701	210	841	0.646
	Volume fraction	0.097	0.358	0.106	0.439	
Mix 250GGBS	Mass (kg)	250	701	210	841	0.649
	Volume fraction	0.119	0.349	0.104	0.428	
Mix 300GGBS	Mass (kg)	300	701	210	841	0.651
	Volume fraction	0.139	0.341	0.101	0.418	
Mix 350GGBS	Mass (kg)	350	701	210	841	0.652

	Volume fraction	0.159	0.333	0.099	0.409	
Mix 400GGBS	Mass (kg)	400	701	210	841	0.652
	Volume fraction	0.177	0.326	0.097	0.400	
Mix 450GGBS	Mass (kg)	450	701	210	841	0.652
	Volume fraction	0.195	0.319	0.095	0.391	
Mix 500GGBS	Mass (kg)	500	701	210	841	0.651
	Volume fraction	0.212	0.312	0.093	0.383	

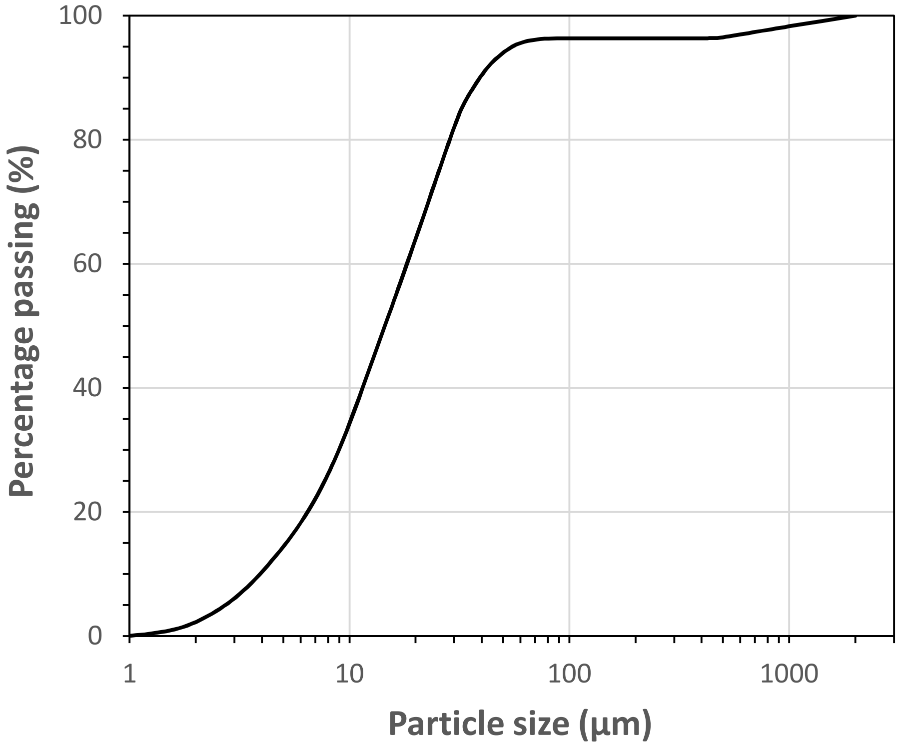

424

425 Fig. 1. Cumulative particle distribution of GGBS

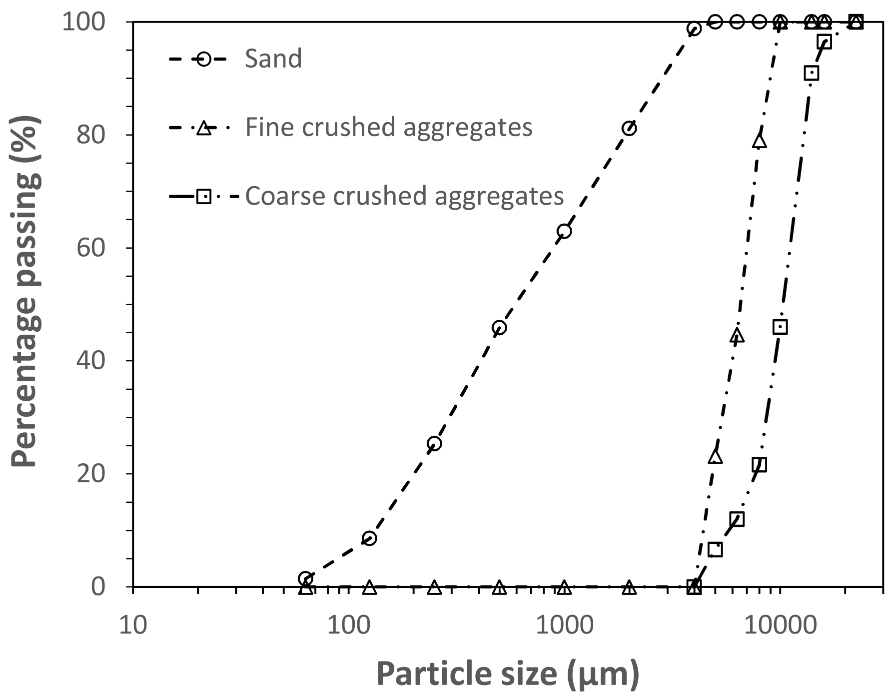

Fig. 2 Particle size distribution of sand and crushed aggregates

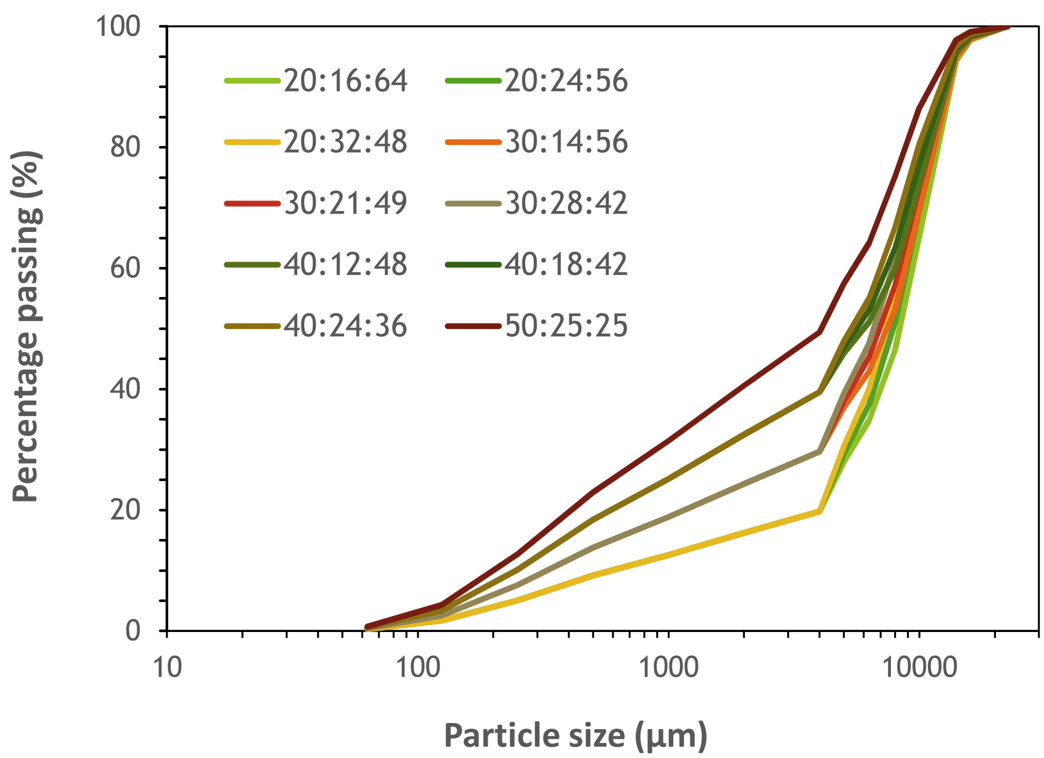

Fig. 3 Particle size distributions for different mix proportions of aggregates (sand/10mm/16.5mm)

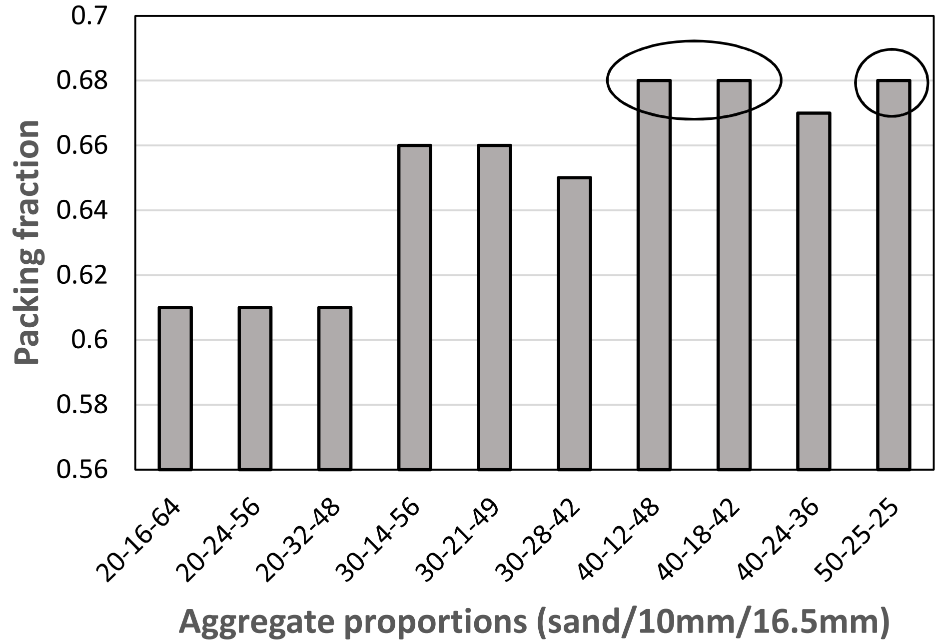

Fig. 4 Packing fraction and void ratio resulted for different proportion of aggregates

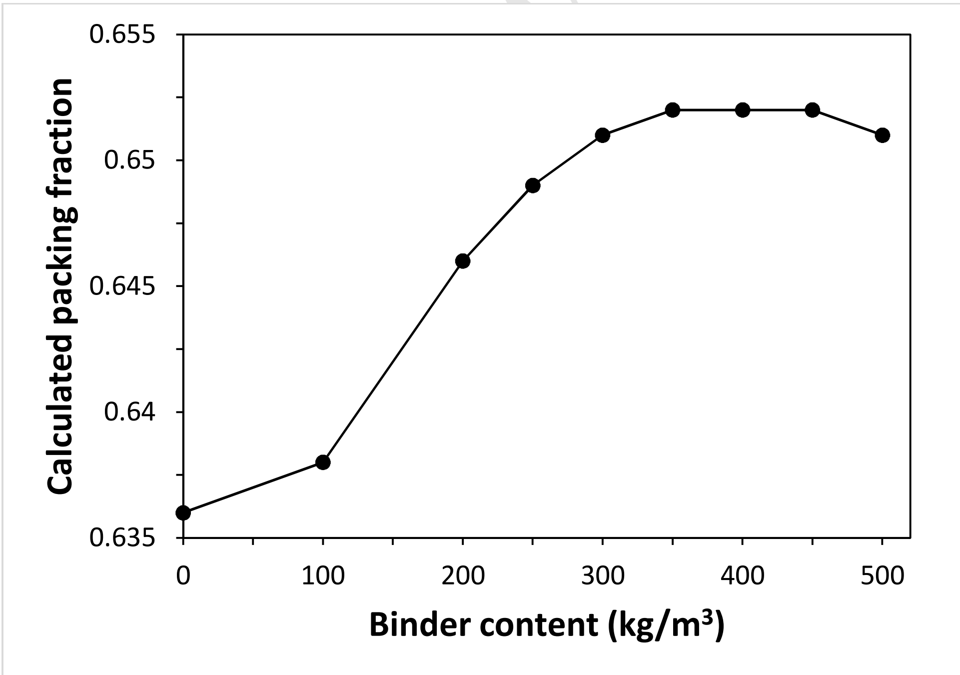

Fig. 5 The relationship between the theoretical packing fraction and binder content of mixes

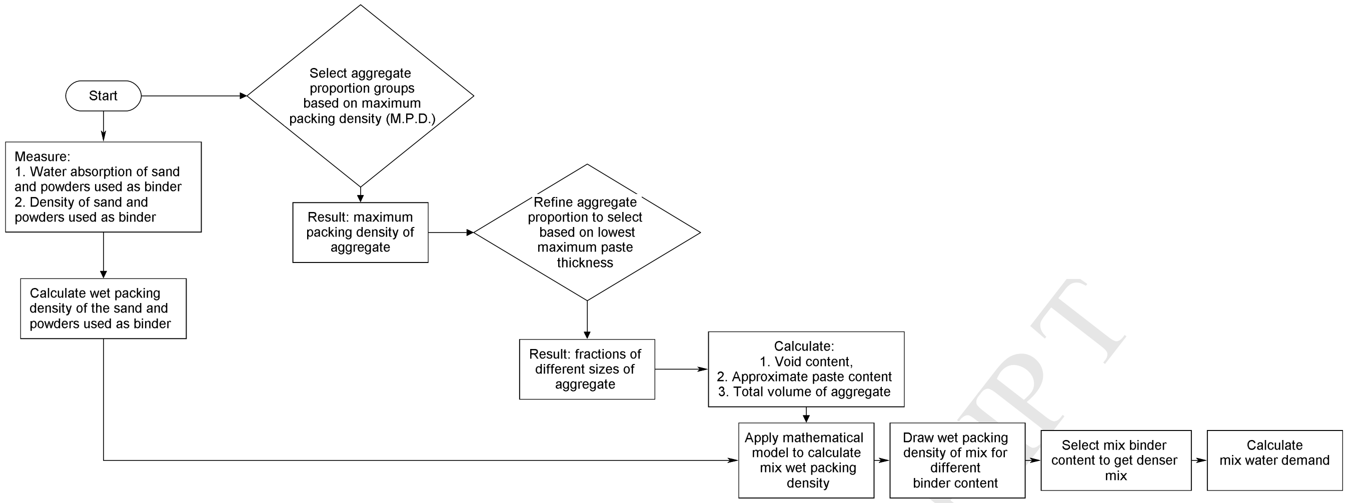

Fig. 6 Mix design procedure for alkali activated concretes

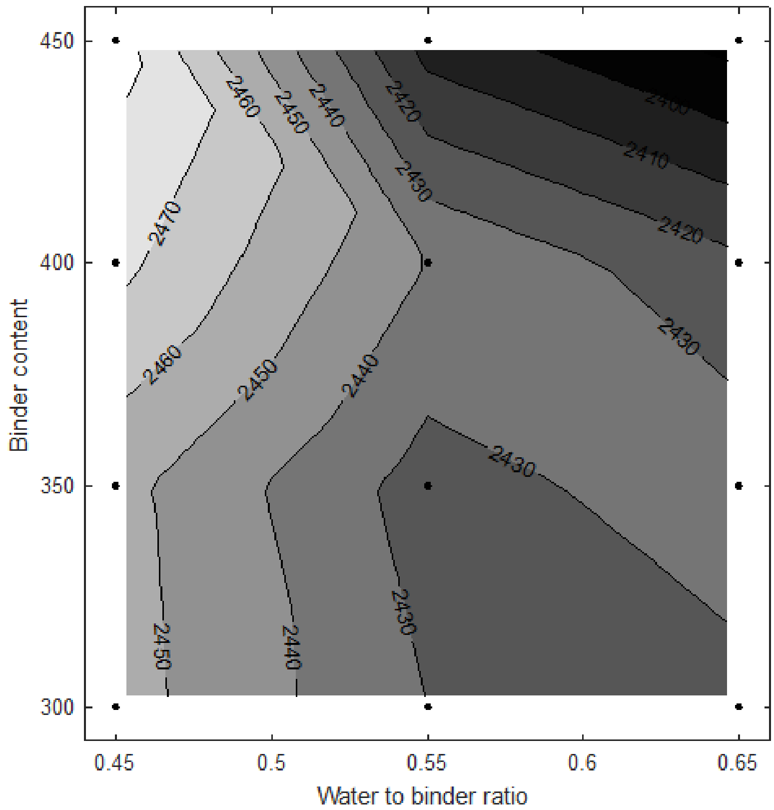

Fig. 7 Contour graph for wet density of mixes made with 4% NaOH & 6% WG, and different binder contents and water to binder ratios

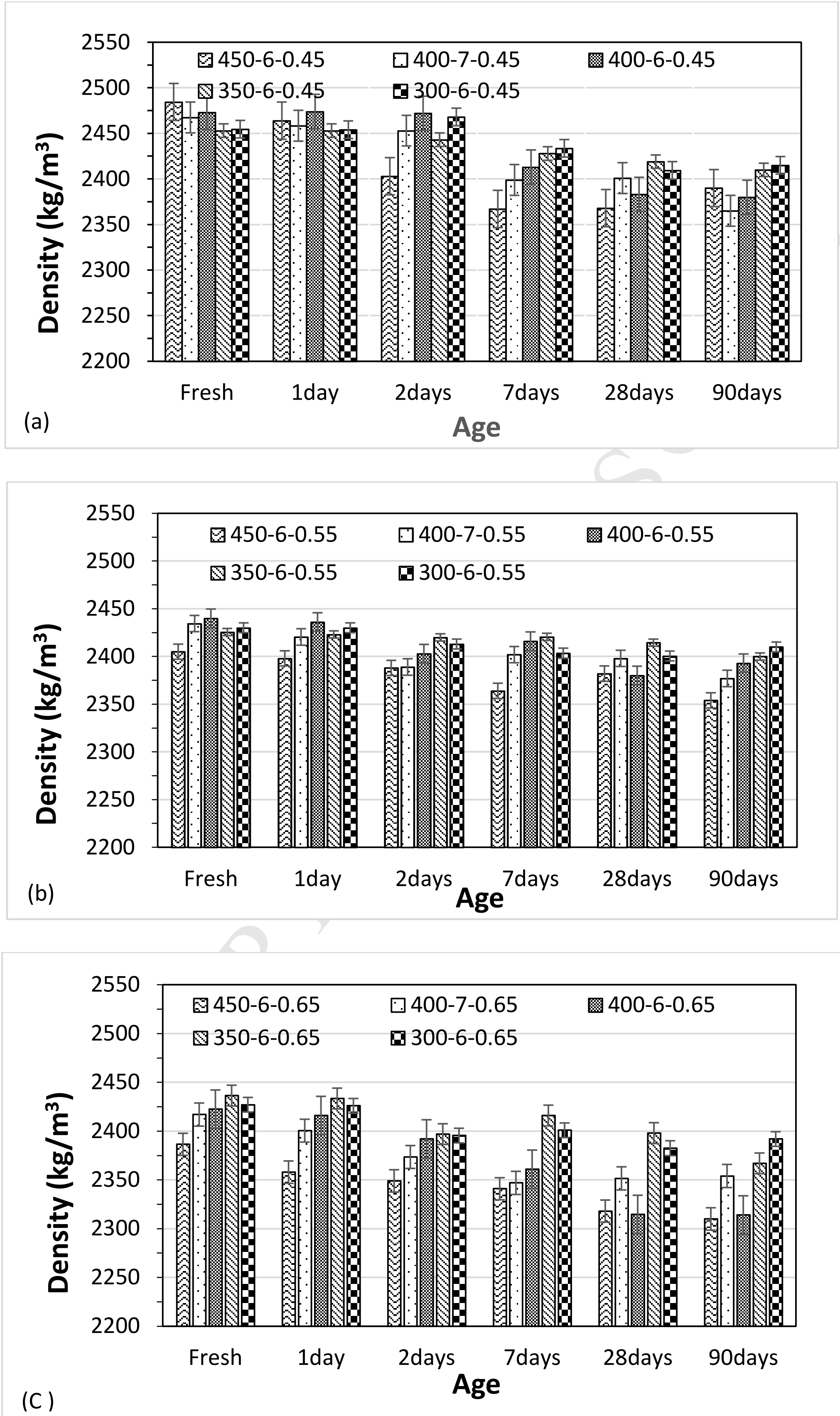
2550
2500
2450
2400
2350
2300
2250
2200
450-6-0.45
400-7-0.45
400-6-0.45
350-6-0.45
300-6-0.45
Density (kg/m³)
Fresh
1day
2days
7days
28days
90days
Age
(a)
450-6-0.55
400-7-0.55
400-6-0.55
350-6-0.55
300-6-0.55
(b)
450-6-0.65
400-7-0.65
400-6-0.65
350-6-0.65
300-6-0.65
(C)

Fig. 8 Density of mixes at different ages (a) Water to binder ratio equal to 0.45; (b) Water to binder ratio equal to 0.55; (c)Water to binder ratio equal to 0.65

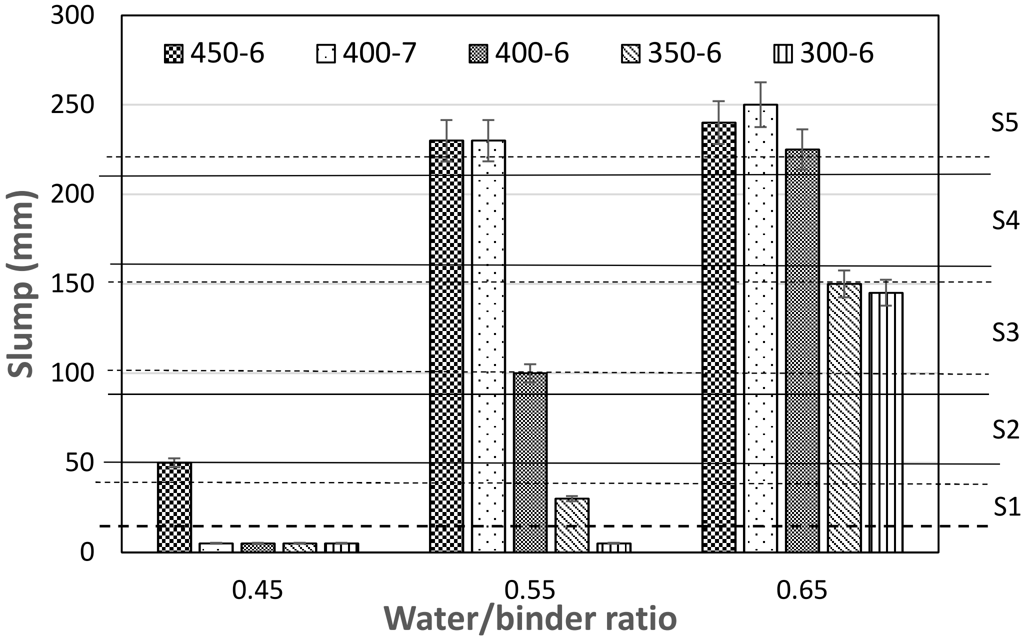

Fig. 9 Slump of mixes with different binder contents and water/binder ratios (dashed and solid horizontal lines show minimum and maximum of slump for each classification)

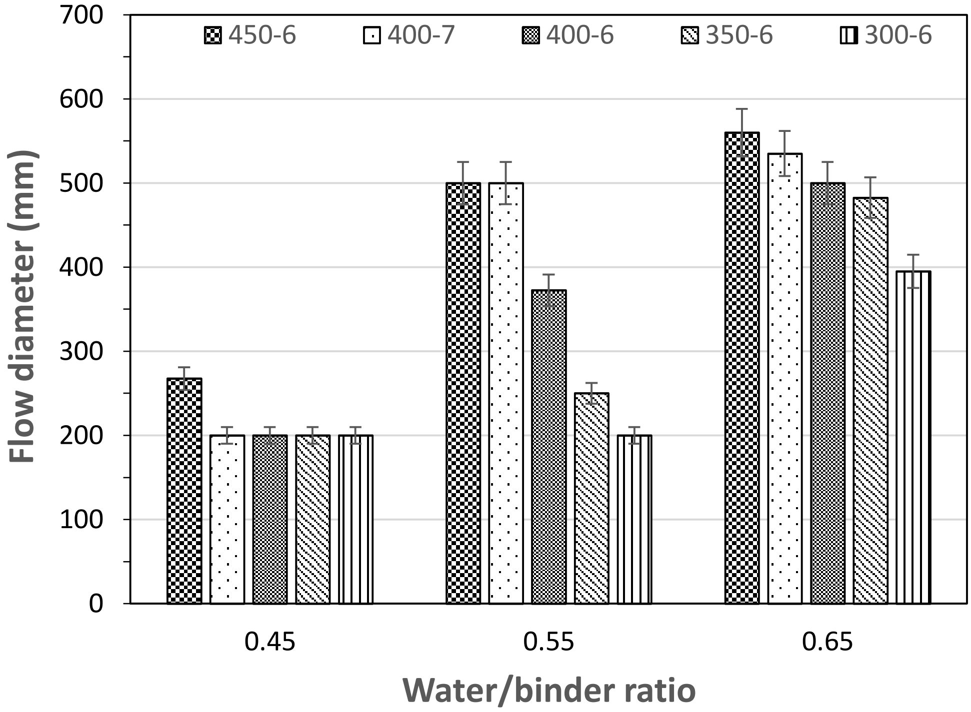

Fig. 10 Flow results for mixes with different binder contents and water/binder ratios

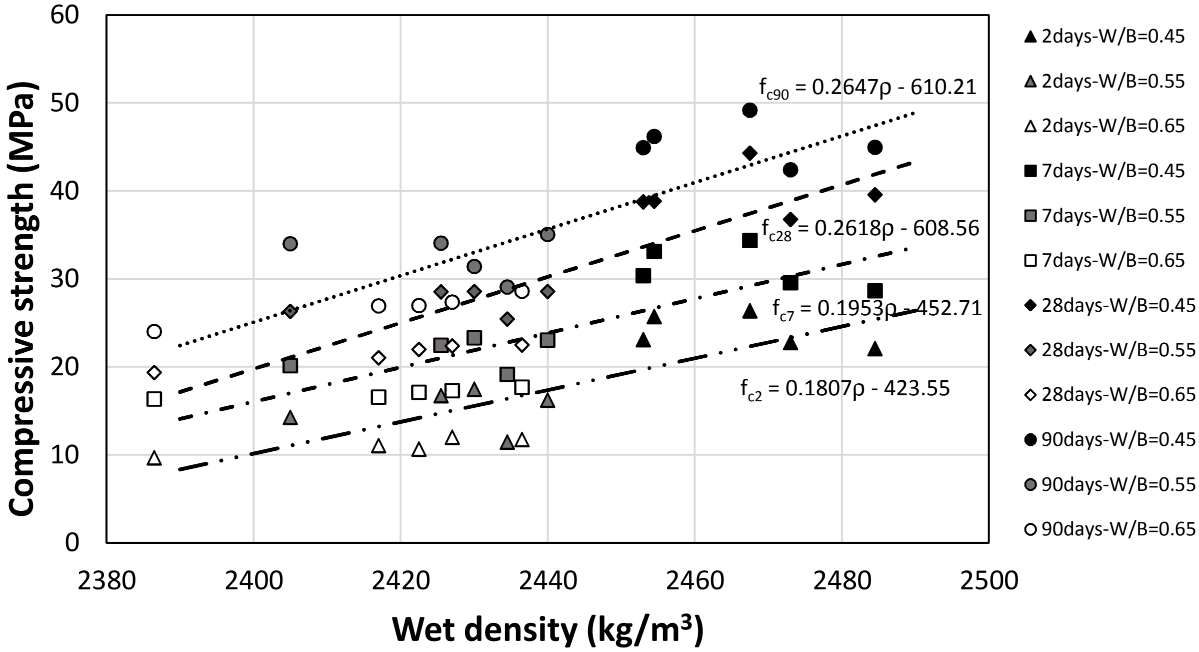

Fig. 11 Compressive strengths at different ages relative to wet density

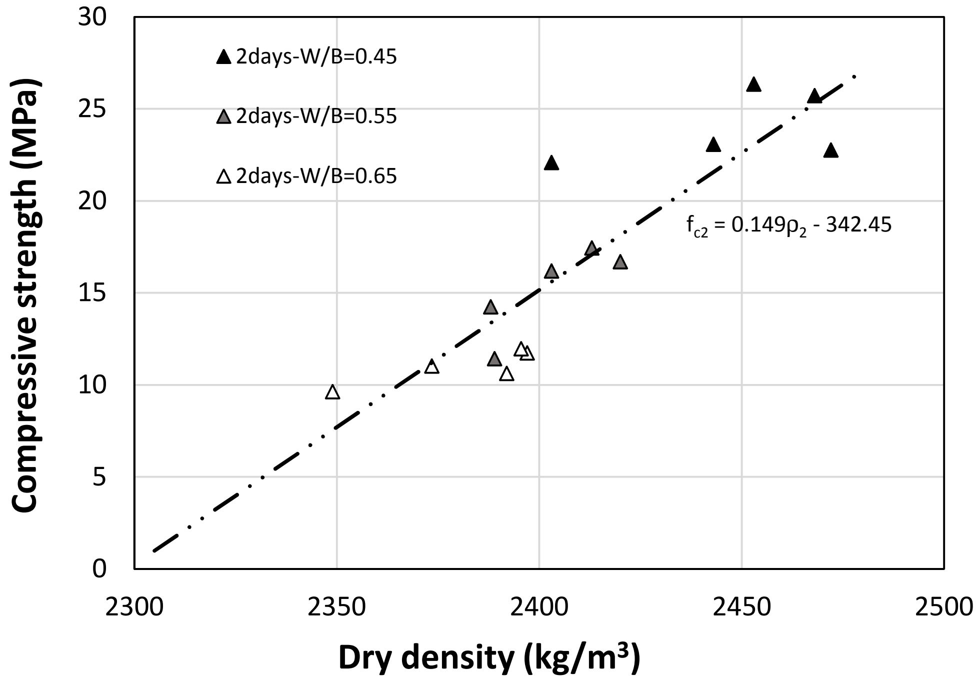

Fig. 12 Compressive strength at 2 days relative to dry density at the same age

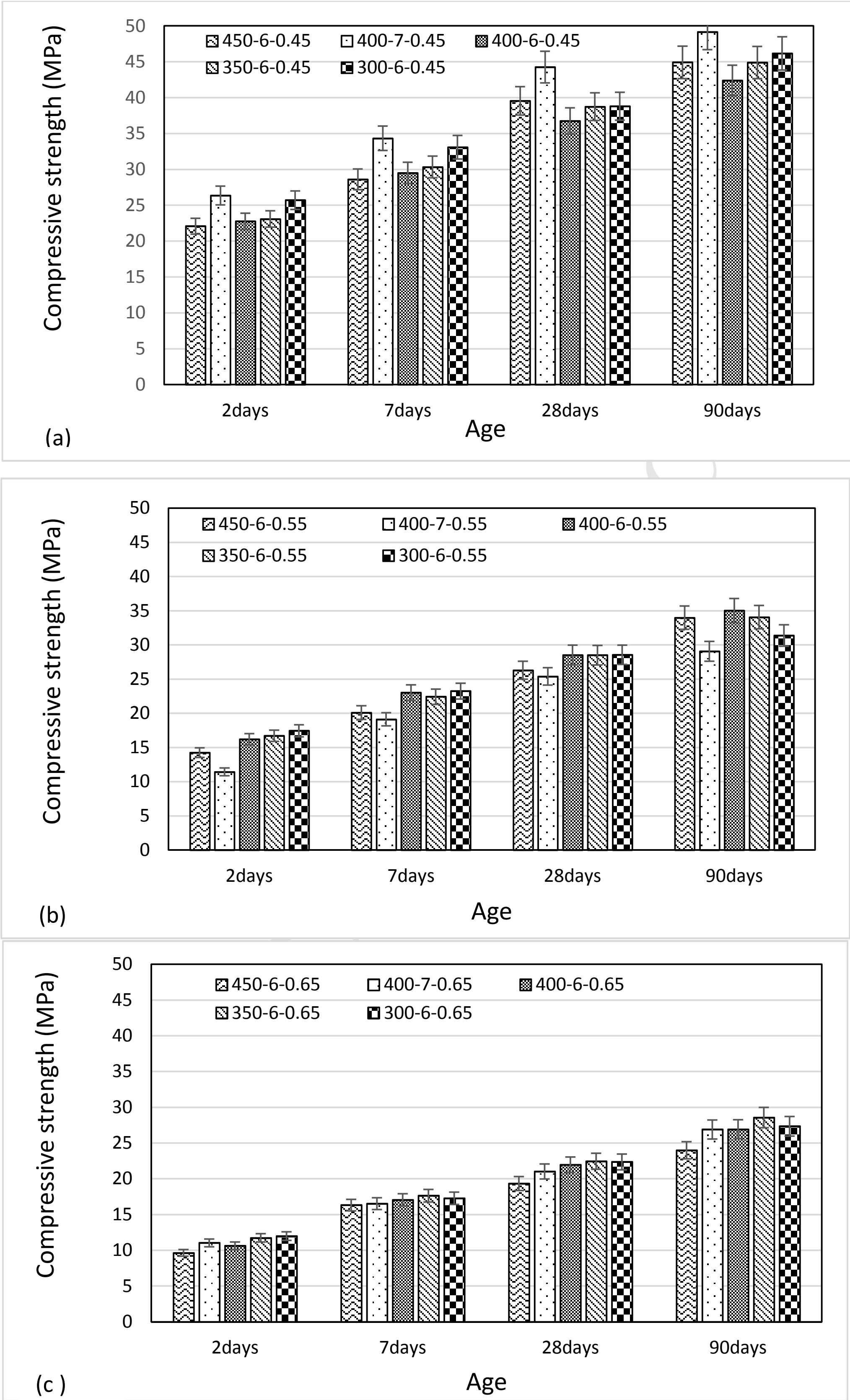

Fig. 13 Compressive strength of different mixes at different ages: (a) Water/binder ratio equal to 0.45; (b) Water/binder ratio equal to 0.55; (c) Water/binder ratio equal to 0.65

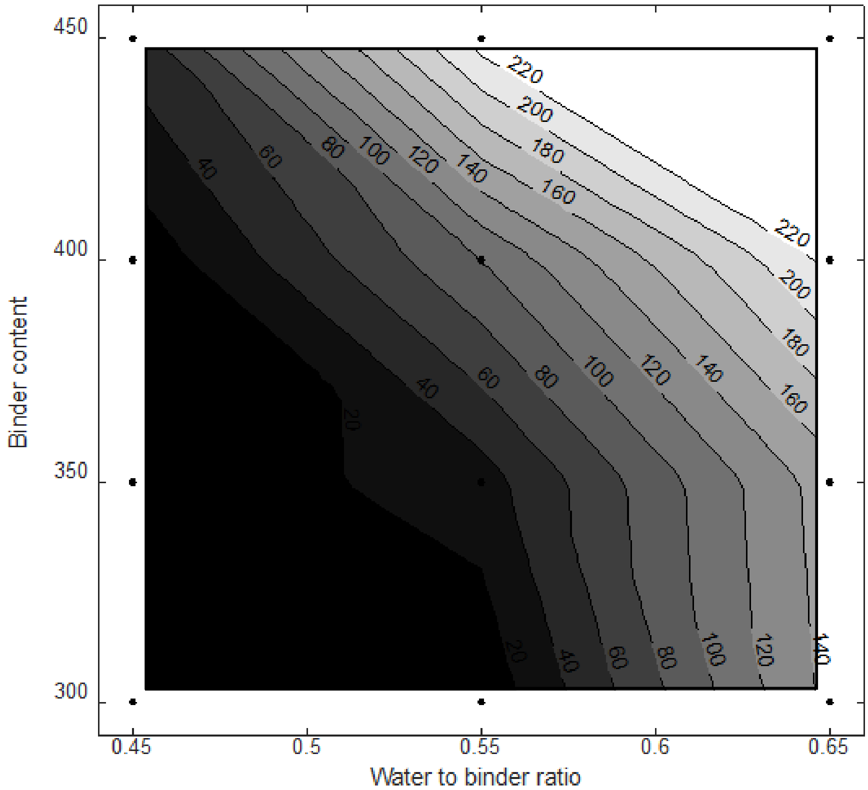

468

(a) Slump

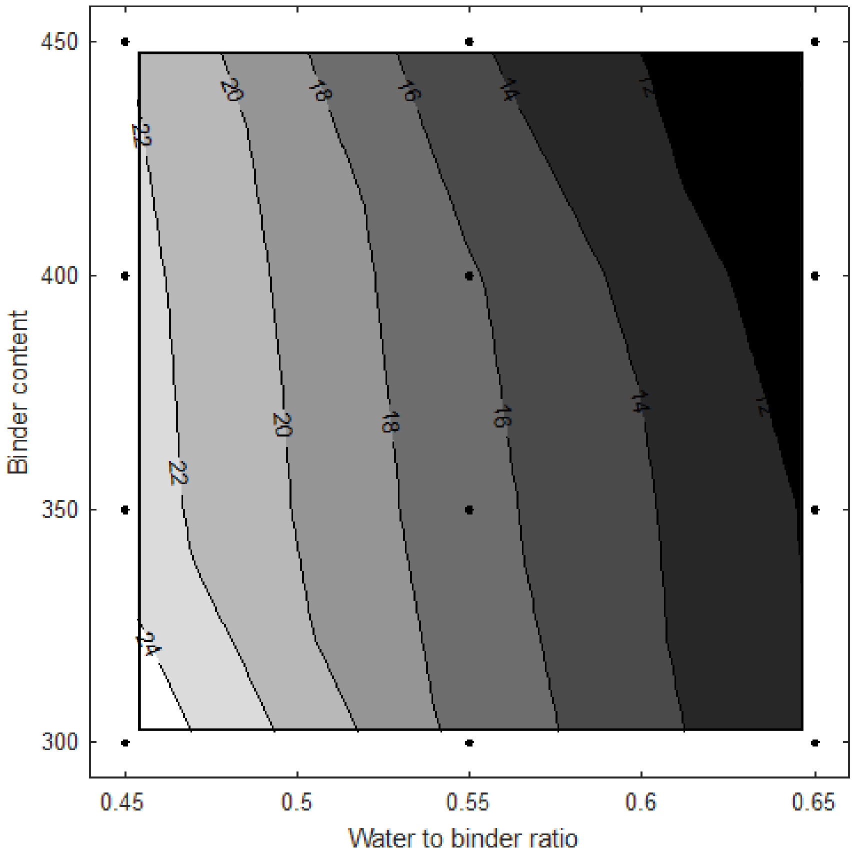

469

(b) 2-day compressive strength (MPa)

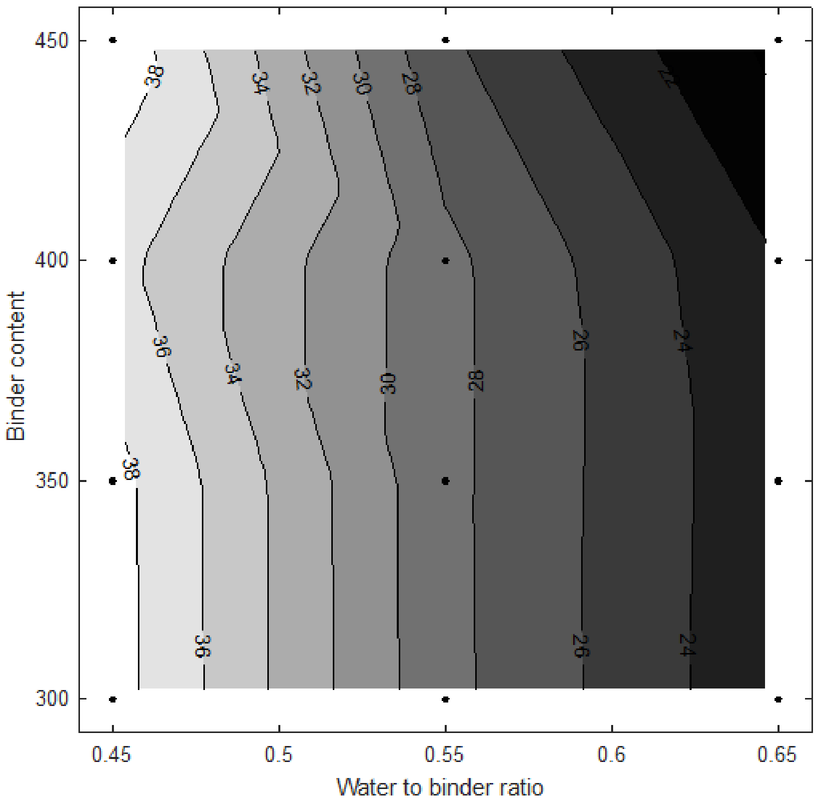

(c) 28-day compressive strength (MPa)

Fig. 14 Contour graphs for workability, early age (2 days) and 28-day compressive strengths of mixes made with the lowest amount of chemical activator (4% NaOH & 6% WG) and different binder contents and water to binder ratios

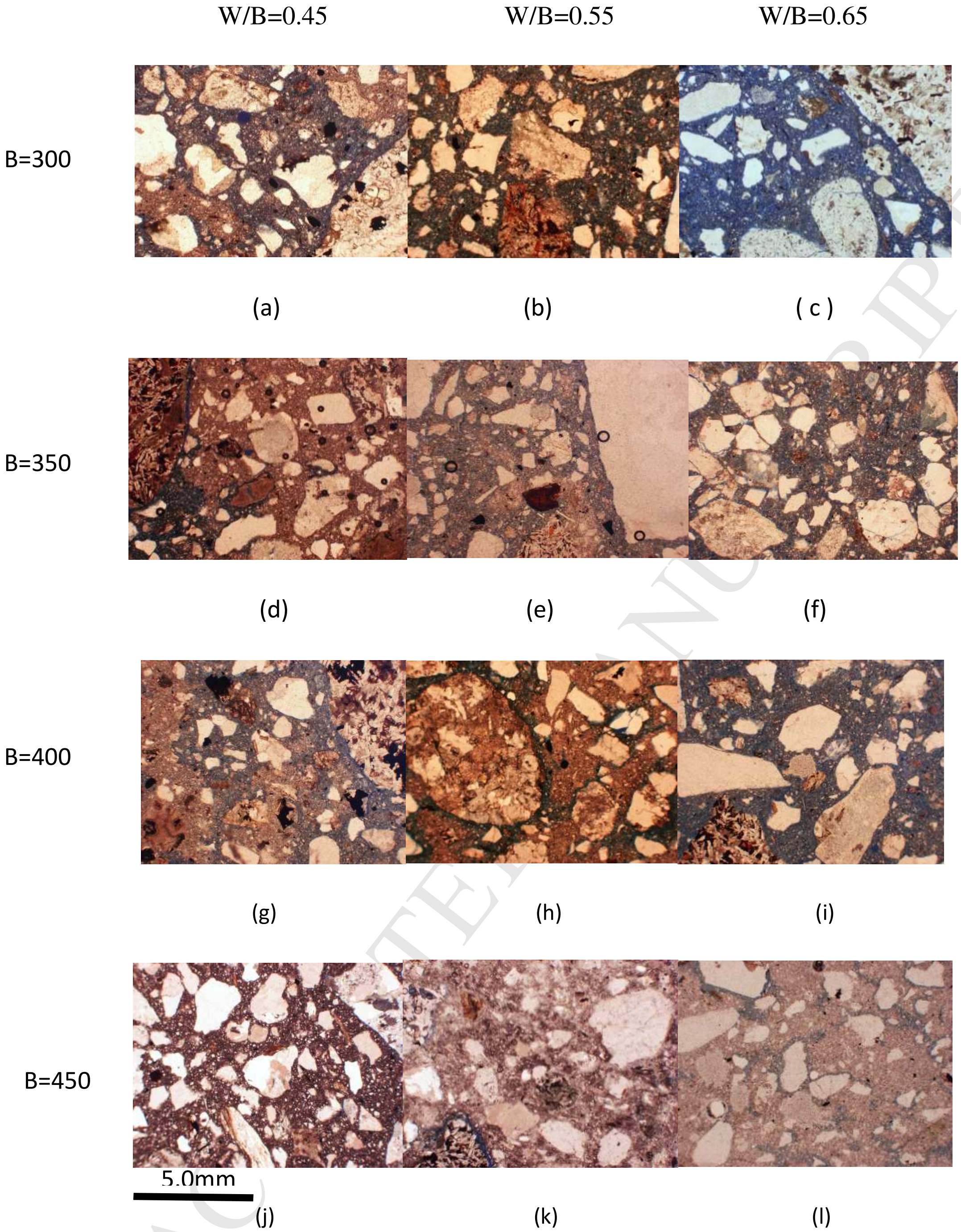

Fig. 15 Thin section micrograph of samples of alkali activated slag concretes with different binder contents (B, kg/m^3) and water to binder ratios. Fields of view for all images are 1.1 x 0.82 cm.

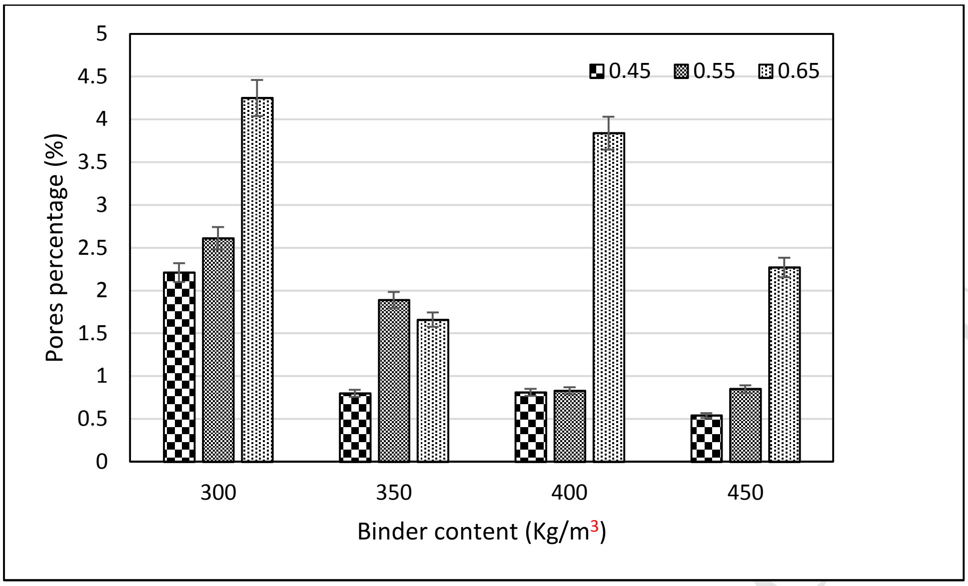

Fig. 16 Pore percentages for mixes with different binder contents, and water/binder ratios as marked

References

Andreasen, A. H. M., (1930) 'Ueber die Beziehung zwischen Kornabstufung und Zwischenraum in Produkten aus losen Körnern (mit einigen Experimenten)', Kolloid-Zeitschrift 50(3), pp 217–228

ASCEM report 174 08_013 Mix Design GGBFS-ASCEM (3) (2014) 'Mix approach for blast furnace slag based AAM', RILEM TC 247-DTA

Bernal S.A., Mejía de Gutiérrez R., Pedraza A.L., Provis J.L., Rodríguez E.D., Delvasto, S. (2011) 'Effect of binder content on the performance of alkali activated slag concretes', Cement and Concrete Research, 41, pp 1-8

Bernal S.A., Mejía de Gutiérrez R., Provis J.L., (2012) 'Engineering and durability properties of concrete based on alkali-activated granulated blast furnace slag/metakaolin blends', Construction and Building Materials, 33, pp 99-108

Bondar D., Lynsdale C.J., Milestone N. B., Hassanie N., and Ramezanianpour A.A., (2011) 'Effect of type, form, and dosage of activators on strength of alkali-activated natural pozzolans', Cement and Concrete Composites, 33(2), pp 251–260

Bondar, D., Ma, Q., Soutsos, M., Basheer, M., Provis, J.L., Nanukuttan, S., (2018) 'Alkali activated slag concretes designed for a desired slump, strength and chloride diffusivity', Construction and Building Materials, under review

BS EN 1097-1 Tests for mechanical and physical properties of aggregates. Determination of the resistance to wear (micro-Deval)

BS EN 12350-2 (2009) Testing fresh concrete Part 2: Slump-test and Part 5: Flow table test

BS EN 12350-3 (2009) Testing hardened concrete Part 3: Compressive strength of test specimens

BS EN 12620: 2013 Aggregates for concrete

BS EN 206 (2013) Concrete: Specification, performance, production and conformity

Collins, F.G., Sanjayan, J.G., (1999) 'Workability and mechanical properties of alkali activated slag concrete', Cement and Concrete Research, 29(3), pp 455-458

de Larrard, F., (1999) 'Concrete Mixture Proportioning: A Scientific Approach', E & FN SPON, London

de Larrard, F., and Sedran, T. (1994) 'Optimization of ultra-high-performance concrete by the use of packing model', Cement Concrete Research, 24(6), pp 997-1009.

Domone P.L.J., and Soutsos M.N. (1994) 'An approach to the proportioning of high strength concrete mixes', Concrete International, 16(10), pp 26–31

Goltermann, P., Johansen, V. and Palbol, L. (1997), "Packing of aggregates: An alternative tool to determine the optimal aggregate mix", ACI Materials Journal, 94(5), pp. 435-443

https://www.elkem.com/silicon-materials/products-and-markets/high-performance-concrete/benefits-of-elkem-microsilica-in-concrete/

Jones M. R., Zheng L., and Newlands M. D., (2002) 'Comparison of particle packing models for proportioning concrete constituents for minimum voids ratio', Materials and Structures, 35, pp 301-309

Kwan A.K.H., and Wong H.H.C. (2008) 'Packing density of cementitious materials: Part 2-packing and flow of OPC+PFA+CSF', Materials and Structures, 41(4), pp 773-784.

Landrou, G., Brumaud, C., Winnefeld, F., Flatt, R.J., Habert, G., (2016) 'Lime as an anti-plasticizer for self-compacting clay concrete', Materials, 9, #330

Lange, F., Mortel, H., and Rudert, V. (1997) 'Dense packing of cement pastes and resulting consequences on mortar properties', Cement and Concrete Research, 27(10), pp 1481-1488

Li L.G., and Kwan A.K.H. (2014) 'Packing density of concrete mix under dry and wet conditions', Powder Technology, 253, pp 514-521.

Li, N., Shi, C., Zhang, Z., Zhu, Z., Hwang, H.J., Zhu, Y., Sun, T., (2018) 'A mixture proportioning method for the development of performance-based alkali-activated slag-based concrete', Cement and Concrete Composites, 93, pp 163–174

Lloyd, N.A., Rangan, B.V., (2010) 'Geopolymer concrete with fly ash'. In: Second international conference on sustainable construction materials and technologies, volume 3, pp. 1493-1504. Ancona, Italy: UWM Center for By-Products Utilization.

McLellan, B.C., Williams, R.P., Lay, J., van Riessen, A., Corder, G.D. (2011) 'Costs and carbon emissions for Geopolymer pastes in comparison to Ordinary Portland Cement', J Cleaner Prod, 19, pp 1080-1090.

Miller K.T., Melant R.M., Zukoski C.F., (1996) 'Comparison of the compressive yield response of aggregated suspensions: Pressure filtration, Centrifugation, and osmotic consolidation', Journal of the American Ceramic Society, 79(10), pp 2545-2556

Miller, S.A., Monteiro, P.J.M., Ostertag, C.P., Horvath, A. (2016) 'Concrete mixture proportioning for desired strength and reduced global warming potential', Construction and Building Materials, 128, pp 410-421

Moini M., Flores-Vivian I., Amirjanov A., and Sobolev K. (2015) 'The optimization of aggregate blends for sustainable low cement concrete', Construction and Building Materials, 93, pp 627-634

Ng, T.S., Foster, S. (2013) ‘Development of a mix design methodology for high-performance geopolymer mortars’, Structural Concrete, 14(2), pp 148-156.

Pavithra, P., Srinivasula Reddy, M., Dinakar, P., Hanumantha Rao, B., Satpathy, B.K., Mohanty, A.N. (2016) ‘A mix design procedure for geopolymer concrete with fly ash’, Journal of Cleaner Production, 133, pp 117-125

Provis J. L., Van Deventer J. S. J., (2014) ‘Geopolymers: structures, processing, properties and industrial applications’, Woodhead, Cambridge, UK, 448 pp.

Rafeet, A., Vinai, R., Soutsos, M., Sha, W., (2017) ‘Guidelines for mix proportioning of fly ash/GGBS based alkali activated concretes’, Construction and Building Materials, 147, pp 130-142

Raj N., Patil S.G., and Bhattacharjee B. (2014) ‘Concrete Mix Design by Packing Density Method’, IOSR Journal of Mechanical and Civil Engineering, 11(2), 34-46.

San Nicolas, R., Provis, J.L., (2015) ‘The interfacial transition zone in alkali-activated slag mortars’, Frontiers in Materials, 2: article #70

Shi, C., Roy, D., Krivenko, P., (2006) ‘Alkali activated cements and concrete’, Taylor & Francis, London/New York, Ch. 8, pages 220-230

Sutcu M., and Akkurt S. (2007) ‘ANN model for prediction of powder packing’, Journal of the European Ceramic Society, 27, pp 641-644

Torres A., Hu J., and Ramos A. (2015) ‘The effect of the cementitious paste thickness on the performance of previous concrete’, Construction and Building Materials, 95, pp 850-859

Wassermann, R., Katz, A., Bentur, A., (2009) ‘Minimum cement content requirements: a must or a myth?’, Materials and Structures 42, pp. 973-982

Ye G., Xin H., Zhu B.-l., Ma B.-g., and Zhu H.-b., (2008) ‘Method for calculating packing density of powder particles in paste with continuous particle size distribution’, Powder Technology, 187, pp 88-93

Yost, J.R., Radlinska, A., Ernst, S., Salera, M. (2013) ‘Structural behavior of alkali activated fly ash concrete. Part 1: mixture design, material properties and sample fabrication’, Materials and Structures, 46(3), pp 435–447

Zheng J., Johnson P.F., and Reed J.S., (1990) ‘Improved equation of the continuous particle size distribution for dense packing’, Journal of the American Ceramic Society, 73(5), pp 1392-1398

Zou R.P., Feng C.L., and Yu A.B., (2001) ’Packing density of binary mixtures of wet spheres’, Journal of the American Ceramic Society, 84(3), pp 504-508

Zou R.P., Xu J.Q., Feng C.L., Yu A.B., Johnston S., and Standish N., (2003) ’Packing of multi-sized mixtures of wet coarse spheres’, Power Technology, 130, pp 77-83

- Rational mix design for AAM concretes can be achieved based on optimising packing fraction of the ingredients.
- AASC designed based on optimising packing fraction of the ingredients has higher slump for a given water content.
- AASC with least dosage of activators can be designed for different workability and concrete grades up to C32/40.
- The binder contents selected in AASC designed based on WPF result in denser mixes as a good indicator of durability.